

AD-776 592

THE EFFECTS OF THICK INTERFACES ON THE  
MECHANICAL PERFORMANCE OF FIBER REIN-  
FORCED COMPOSITES

R. E. Lavengood, et al

Monsanto Research Corporation

Prepared for:

Office of Naval Research  
Advanced Research Projects Agency

March 1974

DISTRIBUTED BY:

**NTIS**

National Technical Information Service  
U. S. DEPARTMENT OF COMMERCE  
5285 Port Royal Road, Springfield Va. 22151

## DOCUMENT CONTROL DATA - R &amp; D

(Security classification of title, body of abstract and indexing annotation must be entered when the overall report is classified)

1. ORIGINATING ACTIVITY (Corporate author)

Monsanto Research Corporation

2a. REPORT SECURITY CLASSIFICATION

Unclassified

2b. GROUP

3. REPORT TITLE

4. DESCRIPTIVE NOTES (Type of report and inclusive dates)

5. AUTHOR(S) (First name, middle initial, last name)

R. E. Lavengood, M. J. Michno, J. D. Fairing

6. REPORT DATE

March, 1974

7a. TOTAL NO. OF PAGES

60

7b. NO. OF REFS

6

8a. CONTRACT OR GRANT NO.

N00014-67-C-0218

b. PROJECT NO.

9a. ORIGINATOR'S REPORT NUMBER(S)

HPC 72-158

c.

9b. OTHER REPORT NO(S) (Any other numbers that may be assigned this report)

d.

10. DISTRIBUTION STATEMENT

Approved for public release; distribution unlimited

11. SUPPLEMENTARY NOTES

12. SPONSORING MILITARY ACTIVITY

Office of Naval Research  
Washington, D. C.

13. ABSTRACT

Techniques are described which permit the application of very uniform thin epoxy coatings on boron or 5 mil diameter glass fiber. These thick interfaces improve the transverse strength and interlaminar shear strength of glass/epoxy composites by as much as 60% and 35% improvements are typical for boron/epoxy composites. Flexural and torsional fatigue strengths of both materials are improved by 1 to 3 orders of magnitude. The resistance of composites to boiling water is also dramatically improved. After a 2 hour boil, thick interface samples retain more than 80% of their original transverse strength while control samples retain only 65 to 75%.

Reproduced by  
NATIONAL TECHNICAL  
INFORMATION SERVICE  
U S Department of Commerce  
Springfield VA 22151

14 KEY WORDS	LINK A		LINK B		LINK C	
	ROLE	WT	ROLE	WT	ROLE	WT
innerface fatigue strength fiber reinforced composites water resistance shear strength glass fiber boron fiber						

THE EFFECTS OF THICK INTERFACES ON THE MECHANICAL  
PERFORMANCE OF FIBER REINFORCED COMPOSITES

by

R. E. Lavengood, M. J. Michno, J. D. Fairing

March 1973  
1974

MONSANTO/WASHINGTON UNIVERSITY ASSOCIATION  
HIGH PERFORMANCE COMPOSITES PROGRAM  
SPONSORED BY ONR AND ARPA  
CONTRACT NO. N00014-67-C-0218, ARPA ORDER 876  
ROLF BUCHDAHL, PROGRAM MANAGER

MONSANTO RESEARCH CORPORATION  
800 NORTH LINDBERGH BOULEVARD  
ST. LOUIS, MISSOURI 63166

## FOREWORD

The research reported herein was conducted by the staff of Monsanto/Washington University Association under the sponsorship of the Advanced Research Projects Agency, Department of Defense, through a contract with the Office of Naval Research, N00014-67-C-0218 (formerly N00014-66-C-0045), ARPA Order No. 876, ONR contract authority NR 356-484/4-13-66, entitled, "Development of High Performance Composites."

The prime contractor is Monsanto Research Corporation. The Program Manager is Dr. Rolf Buchdahl (Phone 314-694-4721).

The contract is funded for \$7,000,000 and expires 30 June, 1974.

1.

# THE EFFECTS OF THICK INNERFACES ON THE MECHANICAL PERFORMANCE OF FIBER REINFORCED COMPOSITES

R. E. Lavengood, M. J. Michno, and J. D. Fairing

## Introduction

It is well known that interfacial failure frequently initiates fracture in fiber-reinforced composite materials (1). Such failures are a natural result of the mismatch in properties of the fiber and the matrix material. In most high performance composites the difference in moduli of the two phases is a factor of ten or more. This leads to load induced stress and strain concentrations in the vicinity of the interface. These effects are frequently superposed onto existing shrinkage stresses which result from a change in temperature and a large difference in the coefficient of thermal expansion of the two phases. This combination of interfacial stresses is often responsible for initiating composite failure.

Coating the fibers with a thin layer of a soft, deformable material should reduce the stresses in the matrix around the fibers and thereby improve off-axis performance. An earlier finite element analysis of such composites, however, produced discouraging results. That study considered a linear elastic model of a composite containing rigid inclusions coated with a soft interlayer and predicted only marginal improvements in ultimate properties of the composite (2). From this study it seemed likely that a coating with nonlinear deformational characteristics might be more beneficial. Another aspect

not considered in the above study is the effect of eliminating the near-infinite stress concentration that results when the matrix shrinks around fibers which are in contact with each other. These concepts are not amenable to computer evaluation so a model study was designed to experimentally determine the effects of a thick, relatively soft interlayer on the performance of unidirectional fiber reinforced composites.

The improvements which are expected should be primarily in transverse and off-axis properties which are controlled by the matrix and the interface. The composites will be evaluated on the basis of transverse strength, water resistance, interlaminar shear strength, and torsional fatigue resistance. The effect of innerlayer thickness will be determined by evaluating innerlayers whose thicknesses are 1%, 2% and 4% of the radius of the fiber. The composite system chosen for the initial phase of the study was glass fiber reinforced epoxy. These results will be supplemented with less extensive data on boron fiber-reinforced epoxy.

#### Specimen Preparation

The fibers used are 4 mil diameter, "E" glass with A-1100 coupling agent applied by the manufacturer, (DeBell and Richardson), and 4.5 mil boron fiber from United Aircraft. The innerlayer coatings are applied to the fiber with the apparatus shown schematically in Figure 1. The fiber supply spool, on the left, is driven by a servo motor, and the speed

is automatically regulated to keep the "trolley car" weight at a constant height. The net weight of the "trolley car" assembly is 50 grams so the tension in the fiber is about 25 grams. The fiber passes through a 180°C preheating tube to reduce surface moisture after which it is coated with a resin solution. Recipes used for the different innerlayer thicknesses are given in Table I.

The first drying tower strips off the solvent and advances the cure of the resin enough that the innerlayer is not permanently distorted as the fiber passes over the pulleys between the first and second towers. Curing the innerlayer is completed in the three subsequent towers. Typical temperatures in the towers are 150°C at the entrance and 280°C at the exit. Sojourn time is about 15 seconds per tower.

The fiber coating speed is nominally 32 feet per minute. This rate, however, was adjusted as necessary to maintain the desired innerlayer thickness. Experiments show that, over the range investigated in this study, the thickness of innerlayer deposited by a given recipe is directly proportional to both the viscosity of the solution and the fiber speed. The solution viscosity increases throughout the day, reflecting the increasing molecular weight of the dissolved resin. However, if the innerlayer deposited at a particular time is thicker than planned the speed is decreased by an amount proportional to the desired reduction in thickness. Once the



proper thickness is achieved, it may be maintained very accurately by adjusting fiber speeds such that the product of coating speed and solution viscosity remains constant. Innerlayer thickness is monitored by determining the weight of resin deposited on the fiber. This is determined with conventional thermal gravimetric analysis apparatus. With proper attention, the thickness can readily be controlled to  $\pm 5\%$  of the desired values. Microscopic examination is used to insure that the innerlayer is deposited in a uniform and concentric manner on the fiber. Details of the microscopy techniques are given in Appendix II. Figure 2 is a cross section of an innerlayered glass fiber which shows the uniformity of the coating.

Torsional fatigue and interlaminar shear specimens are prepared by filament winding a specimen similar to an NOL ring. The outside diameter is 6" and the thickness is 1/8" as usual. The width, however, is also 1/8" instead of the customary 1/4". This minor modification was made to conserve fiber. All other composites are fabricated by a hand alignment technique which consists of orienting the fibers, impregnating, "B" staging, and then molding. More explicit details of this process are given in reference 3. The matrix resin, Shell Epon 828 plus 20 parts per hundred Shell Curing Agent Z, is "B" staged at 40°C for 18 hours and then cured at 100°C for 30 minutes followed by 1-1/2 hours at 180°C. Unidirectional rods were prepared by placing a predetermined weight of fibers in a glass tube, vacuum impregnating, then "B" staging and curing as above.

#### Test Results

Transverse strength is measured in a three-point flexural test. Four specimens of each type are tested and then additional

specimens are run until the relative standard error of the mean is less than 5%. Water resistance is determined by running similar tests on samples which have been boiled in water for 2 hours and then allowed to equilibrate at room temperature for 1 hour. The combined results of these two test series are shown graphically in Figure 3. For the dry samples, the presence of an innerlayer increases the transverse strength from about 6 ksi to nearly 10 ksi and the two percent thickness is optimum. The increase in the ultimate strain of these transverse composites may be even more important than the improved strength. The structural utility of crossplied composites is frequently limited by the low strain capacity of off-axis or transverse plies (4). In these situations composite performance should be greatly improved by using innerlayered fibers.

Figure 3 shows that all the samples lose strength upon exposure to water. While the control material loses 40% of its original strength, the 1, 2 and 4 percent innerlayered samples lose only 31%, 6% and 25%, respectively. As before, all the interlayers are beneficial, and the intermediate thickness is the most desirable. These results again suggest that crossplies made with innerlayered fibers should have greatly improved properties.

Electron scanning photomicrographs of the fracture surfaces reveal dramatic differences between the control and the innerlayered samples. In Figure 4 a magnified view of a single fiber

on the fracture surface of a control sample shows that failure occurred at the glass/resin interface and there is almost no resin adhering to the glass. This is typical for brittle matrix composites (1). Figure 5 shows a comparable fiber on the fracture surface of an innerlayered sample. In this case the fracture has occurred away from the fiber surface and the fiber is still covered with polymer. Furthermore, the residual polymer shows signs of considerable flow, drawing, and tearing. These are all energy absorbing processes which should retard crack propagation and lead to improved composite toughness and strength.

The interlaminar shear strength of these materials was measured by the conventional short beam flexural method. The test specimen is a 0.65 inch long arc from the filament wound ring. The results in Table 2 show that the control material has a shear strength of about 6.5 ksi while all the innerlayered samples have strengths greater than 9 ksi. The difference between the innerlayered samples is not significant, but the trend favors the thinner coating. Interlaminar shear is one of the more common failure modes in the vicinity of attachments, so strength increases of this magnitude could be quite important in structural composites.

The final test in the preliminary series was torsional fatigue. This is a constant maximum stress adaptation of a fatigue test developed at Naval Ordnance Laboratory. The apparatus is shown schematically in Figure 6. The test specimen is half of a filament-wound ring. One end of the specimen is clamped in a rigid torque transducer and the other end is twisted back and forth, out of the plane of the ring. The twist angle is continually adjusted to maintain constant

maximum torque. Fatigue life is arbitrarily defined as the number of cycles required to produce a 20% change in the twist angle. This test was chosen, not only because it represents a meaningful off-axis loading mode, but also because of the type of failure it produces. The applied torque produces a state of shear in the midsection of the specimen. This shear is not interlaminar as in the earlier quasi-static tests, but is in a plane perpendicular to the axis of the fibers. In this test, failure occurs in the midsection of the ring and results in cracks along fibers. These cracks propagate around and between fibers in the manner shown in Figure 7. This polished cross-section of a failed specimen shows that cracks run preferentially along the fiber/matrix interface and secondarily through the matrix between fibers.

The results of the torsional fatigue tests are shown in Figure 8. The data points for all the innerlayered samples lie in a narrow band and there is no significant effect of thickness. All the innerlayered samples, however, have fatigue lives at least an order of magnitude greater than the control samples.

The property improvements sighted above are all at room temperature. The innerlayer material has a relatively low glass transition temperature so the strength properties of innerlayered composites should decrease with increasing temperature. Shear

modulus,  $G_{23}$ , and mechanical damping at about 1 Hz were evaluated from room temperature to 170°C, with a torsion pendulum. The specimens were only about 10 fiber diameters thick, so the absolute values of the data are not meaningful. The relative values, shown in Figure 9, indicate a transition at 70°C, and another at 165°. The higher temperature phenomenon reflects the glass temperature of the matrix resin so the lower peak must be caused by the innerlayer material. This is quite important because in the bulk this polymer has a glass temperature of about 40°C. This implies that the innerlayer resin has been structurally modified in the coating process. It is, therefore, not possible to characterize the mechanical properties of the innerlayer material by testing cast sheets of similar composition. This observation terminated the attempt to determine quantitatively the effect of innerlayer stiffness.

The influence of innerlayer modulus was, however, studied qualitatively by determining transverse strength of all the composites at a few elevated temperatures. These data are summarized in Figure 10. The strength of all samples with coated fibers decreases dramatically in the vicinity of 70°. Clearly, if this innerlayer concept is to be used in structural composites, the glass temperature of the deformable layer should be greater than the use of temperature.

The above are the results of the study of a model system of 4 mil diameter glass fiber reinforced epoxy. The very

encouraging findings prompted a supplementary set of experiments to evaluate deformable innerlayers in a higher performance composite system. For convenience we chose boron-reinforced epoxy for this phase of the study. We also eliminated to 1% and 4% thicknesses to reduce the number of experiments. Characterization of the effects of a ductile innerlayer on the longitudinal performance of composites reinforced with both continuous and short (i.e., 1/2" long) fibers was added to the off-axis testing.

The transverse strength and water resistance of boron/epoxy composites with and without innerlayers is shown in Figure 11. As with the glass fiber samples, the innerlayered composite has superior dry and wet strength. The 82 percent strength retention for the innerlayered material after 2 hours in boiling water is also higher than the 65 percent for the control material. Torsional fatigue data for the boron/epoxy samples are shown in Figure 12. The two orders of magnitude improvement which results from the addition of the innerlayer is even greater than the corresponding improvement in the glass epoxy samples.

This improvement in fatigue resistance could reflect an increased resistance to crack propagation or higher initial strength of the innerlayered samples. Static shear strength was determined by torsion tests of unidirectional rods. Aluminum stubs were glued to each end of the 1/4" diameter rods to facilitate gripping. The specimens had a free length of



one inch. Tests were run at a constant rate of rotation and applied torque and twist angle were recorded.

Shear stresses and strains were calculated by nonlinear plasticity techniques developed for torsion of solid bars (5). The surface shear stress is given by:

$$\tau = \frac{1}{2\pi r^3} \frac{d}{d\phi} (T\phi^3)$$

where  $r$  is the radius of the specimen

$\phi$  is the twist angle

and  $T$  is the applied torque.

In the linear region this reduces to:

$$\tau = \frac{2T}{\pi r^3} .$$

The corresponding shear strain is given by:

$$\gamma = \tan^{-1} \frac{r\phi}{l}$$

Test results are tabulated in Table 4 and representative stress-strain curves are shown in Figure 13. The shear test employed was developed for uncoated boron reinforced epoxy and is quite adequate for that purpose. However, the very high torque required to break innerlayered samples usually caused some debonding in the glue joint. Such debonding alters the twist angle and makes precise calculation of ultimate shear stresses and strains impossible. As a result, these values

are missing in Table 4. The high torque region of the stress-strain curve bar innerlayered material in Figure 12 is based on sample 2c which fortunately showed no debonding. This particular sample was twice as strong and had 28% greater ultimate strain than the average control material.

The linear region in the initial portion of the shear stress-strain curve is much longer for the innerlayered samples. This results in more than doubling the strain at the proportional limit and a 40% increase in stress. This is accompanied by a 35% decrease in torsional stiffness. Beyond the proportional limit, there is a marked difference in the shape of the stress-strain curves. The non-innerlayered specimens show an instability (i.e., the slope changes sign) while the stress-strain curves for the innerlayered material is continuously rising until fracture. Eliminating this material instability should reduce design problems in load critical situations. The combined transverse and shear data clearly demonstrates the beneficial effects that a deformable innerlayer can have on off-axis properties of these high performance composites.

The next critical question concerns the effect that an innerlayer has on longitudinal properties. The reduction in stress concentrations might be quite beneficial, however, the reduced stress transfer reported by Gaonkar (6) could overshadow



this and cause a net loss in performance. A series of short fiber and continuous fiber samples were prepared for longitudinal evaluation. The dry strength and strength after 72 hours in boiling water are shown in Table 3. For the continuous fiber samples, the addition of an innerlayer causes a slight (i.e., 5%) decrease in initial strength. This deleterious effect is overshadowed by the very significant increase in water resistance. Three days in boiling water causes nearly 40% loss in strength for the control sample, but less than 4% for the innerlayered composites.

The performance of the short fiber samples is quite different. In this case the initial strength of the innerlayered samples is somewhat greater than the control, but exposure to water causes 30% loss in strength for both materials. The net effect is that the innerlayer improves both wet and dry performance, but neither improvement is as great as that of the boiled continuous samples.

The final tests in this study measured the resistance of short boron fiber-reinforced samples to flexural fatigue. Samples are sinusoidally loaded in three point flexure. The amplitude is continually adjusted so that the peak load is constant. Figure 14 shows that over the entire range of this investigation, the fatigue resistance of the innerlayered samples are greater than that of the controls. Figure 15 shows the same data replotted in normalized form. Again the innerlayered samples are better over the entire range.

In summary, these experiments were designed explicitly to determine the effects of a deformable innerlayer on the mechanical performance of unidirectional composites. The results show that for both glass and boron fiber composites such an innerlayer can improve transverse strength, interlaminar shear strength, water resistance, and both flexural and torsional fatigue life. It can be inferred from these improvements that soft innerlayers should also increase the usable strength of crossplied composites.

Future work should be directed both toward utilizing innerlayered composites in practical applications and elucidating the mechanisms responsible for these improvements.

#### Acknowledgments

The author wishes to express his gratitude to Dr. A. S. Kenyon and Mr. J. D. Fairing for their many technical contributions to this study, and to Messrs. J. J. Cornell, C. N. Rasnick, and W. J. Neff for their assistance throughout the experimental phase of the study.

This research was supported by the Advanced Research Projects Agency of the Department of Defense and was monitored by the Office of Naval Research under Contract No. N00014-67-C-0218.

References

1. Ishai, O., Anderson, R. M. and Lavengood, R. E., "Failure-Time Characteristics of Continuous Unidirectional Glass-Epoxy Composites in Flexure," J. of Materials, Vol. 5, March 1970.
2. Matonis, V. A., "An Analytical Evaluation of a Hypothetical Three-Phase Material, Ph.D. Thesis, U. of Conn., 1967.
3. Lavengood, R. E. and Gulbranse, L. B., "The Effect of Aspect Ratio on the Fatigue Life of Short Boron Fiber Reinforced Composites," Polymer Engineering and Science, Vol. 9, No. 5, Sept. 1969.
4. Lavengood, R. E. and Ishai, O., "The Mechanical Performance of Cross-Plied Composites," Polymer Engineering and Science, Vol. 11, No. 3, May 1971.
5. Nadai, A., Theory of Flow and Fracture of Solids, McGraw-Hill, 1950, Chap. 21, Pg. 397.
6. Gaonkar, G. H., "Plane Stress Fields Due to Isolated and Multirows of Inclusion in an Elastic Continuum," D.Sc. Thesis, Washington University, January 1967.

List of Tables

- Table 1. Composition of resin/solvent mixtures used to apply innerlayer coatings.
- Table 2. Interlaminar shear strength of unidirectional glass reinforced epoxy specimens.
- Table 3. Effect of 72 hours in boiling water on longitudinal strength of boron reinforced epoxy.
- Table 4. Shear test results for unidirectional boron/epoxy rods.

TABLE 1

Recipes for Coating Solutions

1% Innerlayer

54 gm Epon 815  
66 gm Versamid-140  
270 ml Acetone  
30 ml Isopropyl Alcohol

2% Innerlayer

75.6 gm Epon 815  
92.4 gm Versamid-140  
270 ml Acetone  
30 ml Isopropyl Alcohol

4% Innerlayer

76.5 gm Epon 815  
93.5 gm Versamid-140  
180 ml Acetone  
20 ml Isopropyl Alcohol

TABLE 2

Interlaminar Shear Strength

<u>Fiber</u>	<u>PSI</u>
Uncoated	6450
V-1	9660
V-2	9330
V-4	9120

TABLE 3

Effect of 72 Hours in Boiling Water  
on Longitudinal Strength of Boron/Epoxy

<u>Reinforcing Fiber</u>	<u>Original Strength (KSI)</u>	<u>After Boil (KSI)</u>	<u>% Retention</u>
Continuous control	289	176	60.8
Continuous innerlayered	274	267	97.5
1/2 inch control	164	121	73.3
1/2 inch innerlayered	182	127	70.1

Table 4

Shear Test Results for Unidirectional Boron/Epoxy Rods

<u>Boron</u>					
Spec. No.	T <sub>pl</sub> <sup>*</sup> (in lb)	T <sub>max</sub> (in lb)	T <sub>pl</sub> (psi)	γ <sub>pl</sub> in/in	G x 10 <sup>6</sup> psi
1B	17	76	4050	.0029	1.40
2B	16	57	3900	.0024	1.60
3B	18	68	4300	.0029	1.51
4B	15	68	3560	.0027	1.30
5B	<u>19</u>	<u>68</u>	<u>4600</u>	<u>.0028</u>	<u>1.64</u>
Average	17	67	4082	.0027	1.49
<u>Coated Boron</u>					
1C	22	-	5200	.0061	.85
2C	28	128	6470	.0059	1.10
3C	26	88 <sup>†</sup>	6130	.0067	.92
4C	22	-	5140	.0069	.75
5C	<u>24</u>	<u>93<sup>†</sup></u>	<u>5710</u>	<u>.0047</u>	<u>1.23</u>
Average	24	103	5730	.0060	.97

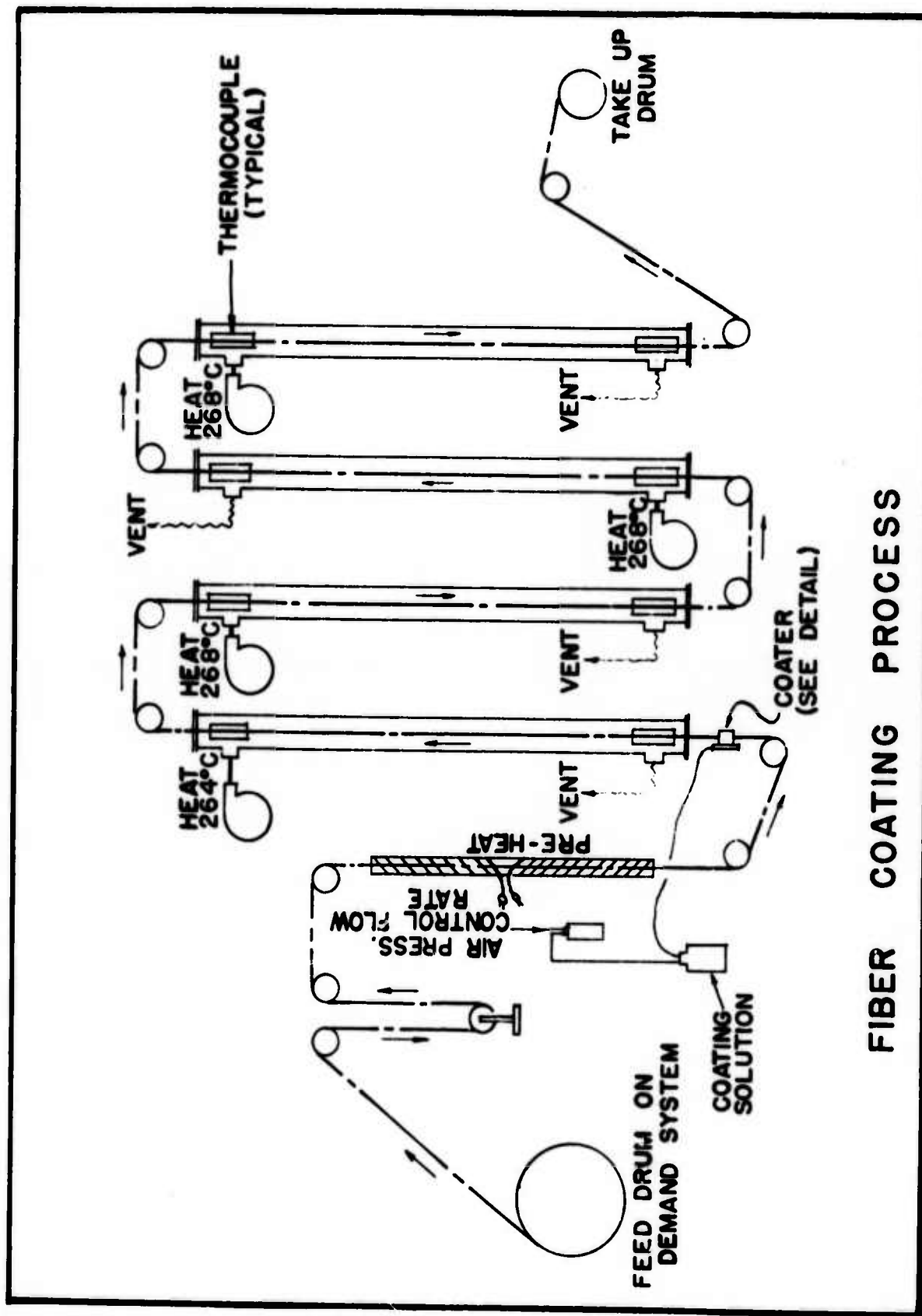
\*Subscript pl denotes proportional limit.

†Max. observed may be low due to glue joint failure.

List of Figures

- Figure 1. Schematic representation of fiber coating apparatus.
- Figure 2. Cross-section of innerlayered fiber showing uniformity of coating.
- Figure 3. Transverse strength of glass fiber reinforced composites before and after 2 hours in boiling water.
- Figure 4. Scanning electron micrograph of fracture surface of transverse composite reinforced with uncoated fibers.
- Figure 5. Scanning electron micrograph of fracture surface of transverse composite reinforced with inner-layered fibers.
- Figure 6. Schematic illustration of torsional fatigue tester.
- Figure 7. Polished cross-section of failed torsional fatigue specimen showing cracks for propagating around and between fibers.
- Figure 8. Torsional fatigue life vs. applied stress for glass fiber reinforced samples.
- Figure 9. Dynamic modulus and damping as a function of temperature. Data were taken with a torsion pendulum at about 1 Hz.
- Figure 10. Transverse strength of composites at temperatures above and below the glass temperature of the innerlayer.
- Figure 11. Transverse strength of boron fiber reinforced composites before and after 2 hours in boiling water.
- Figure 12. Torsional fatigue life vs. applied stress for boron fiber reinforced samples.
- Figure 13. Typical shear stress-strain curves for boron/epoxy composites.
- Figure 14. Flexural fatigue life vs. applied load for short boron fiber reinforced epoxy.
- Figure 15. Flexural fatigue life vs. normalized applied load for short boron fiber reinforced epoxy.





## FIBER COATING PROCESS

Figure 1. Schematic representation of fiber coating apparatus

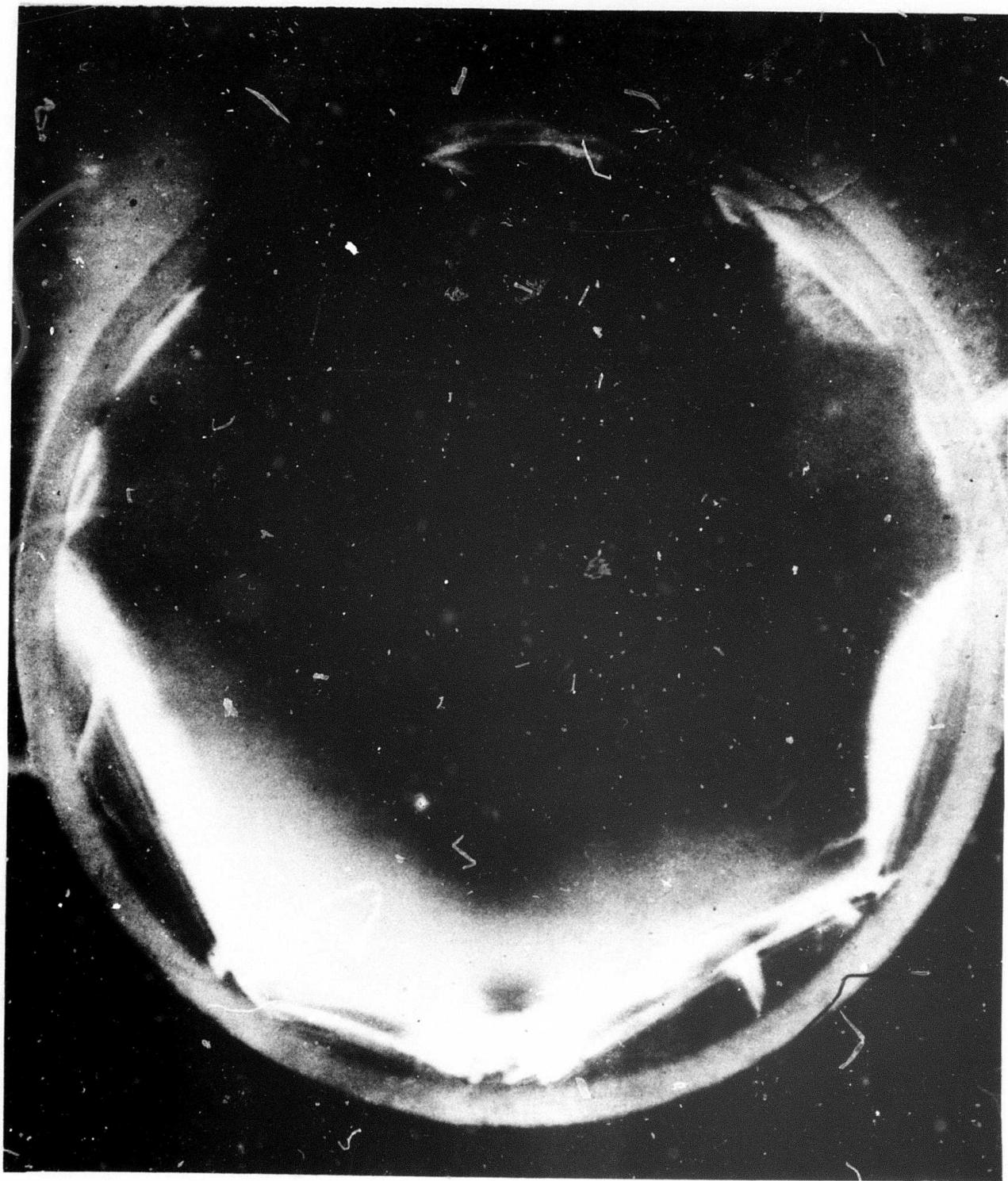
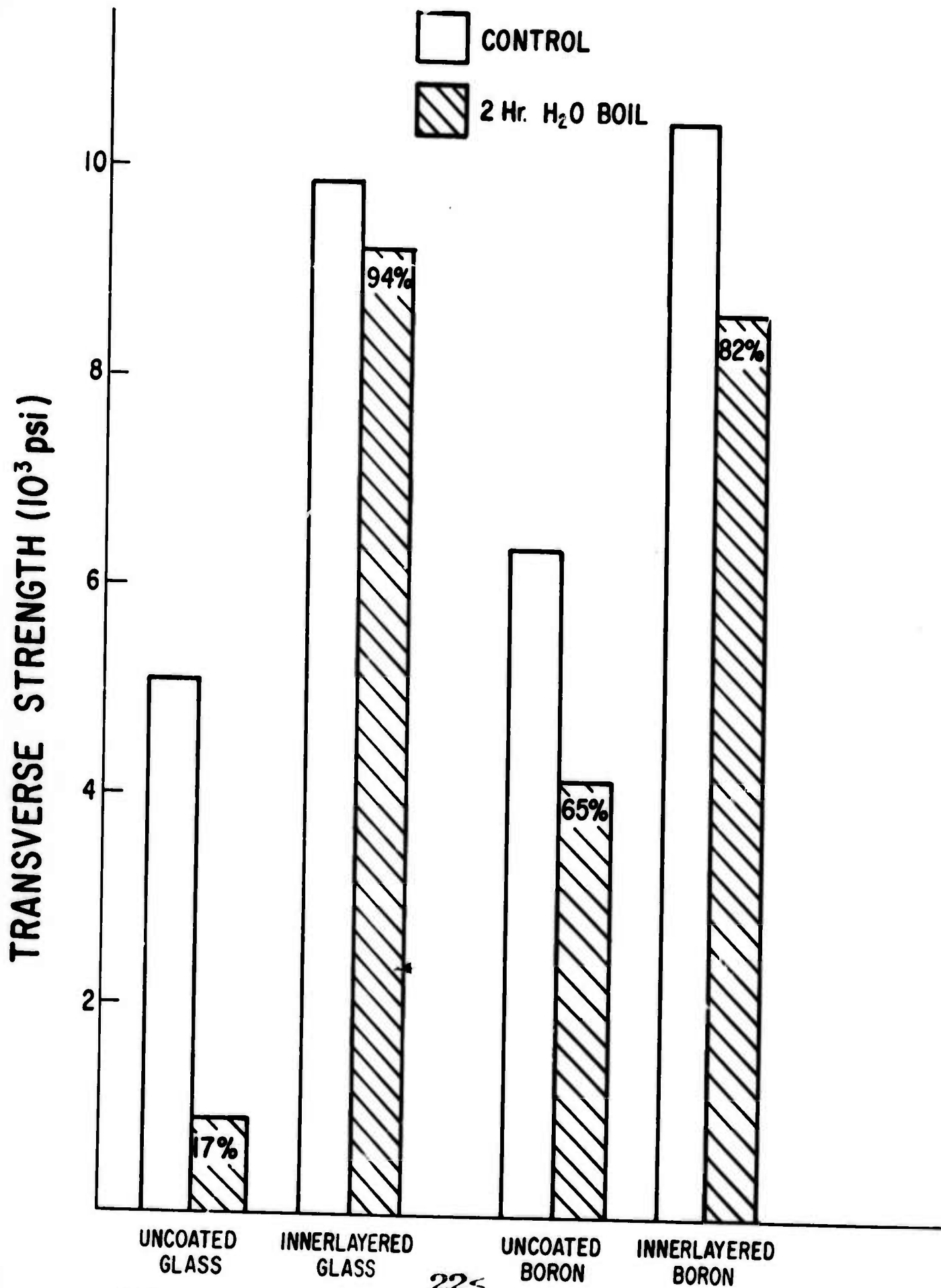


Figure 2. Cross-section of innerlayered fiber showing  
uniformity of coating



22<  
Figure 3. Transverse strength of glass fiber reinforced composites before and after 2 hours in boiling water

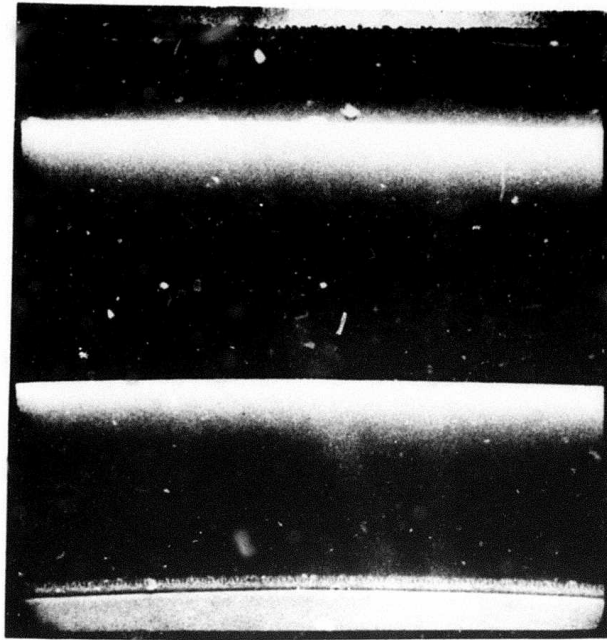


Figure 4. Scanning electron micrograph of fracture surface of transverse composite reinforced with uncoated fibers

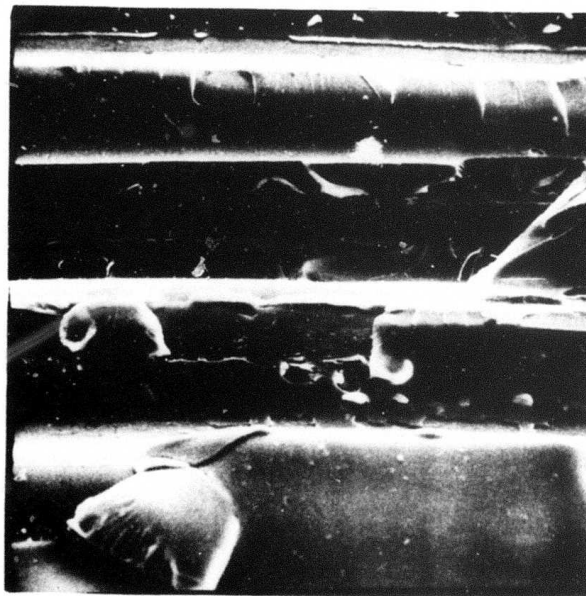
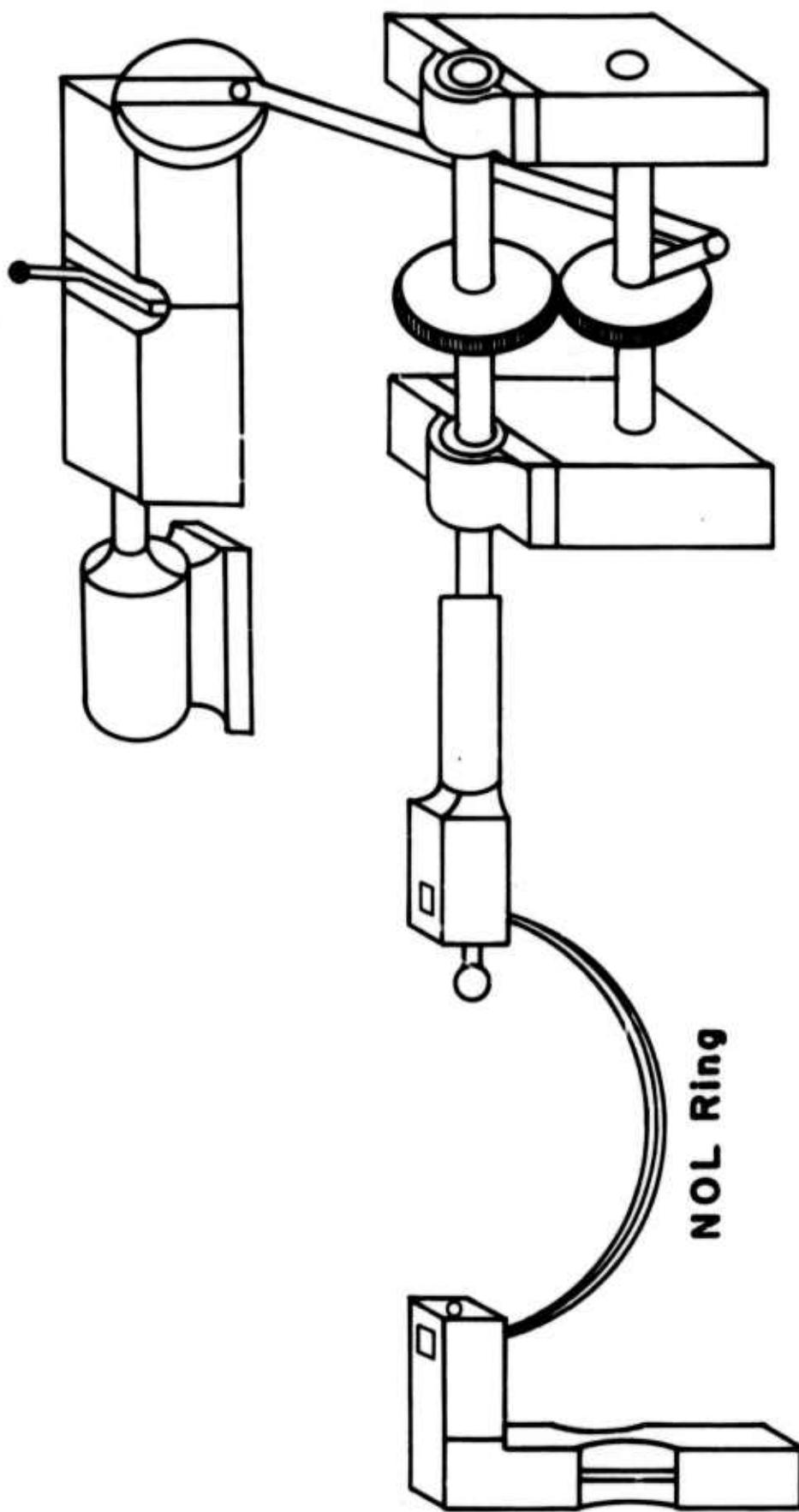


Figure 5. Scanning electron micrograph of fracture surface of transverse composite reinforced with inner-layered fibers

**Variable Speed Drive**



**NOL Ring**

Figure 6. Schematic illustration of torsional fatigue tester

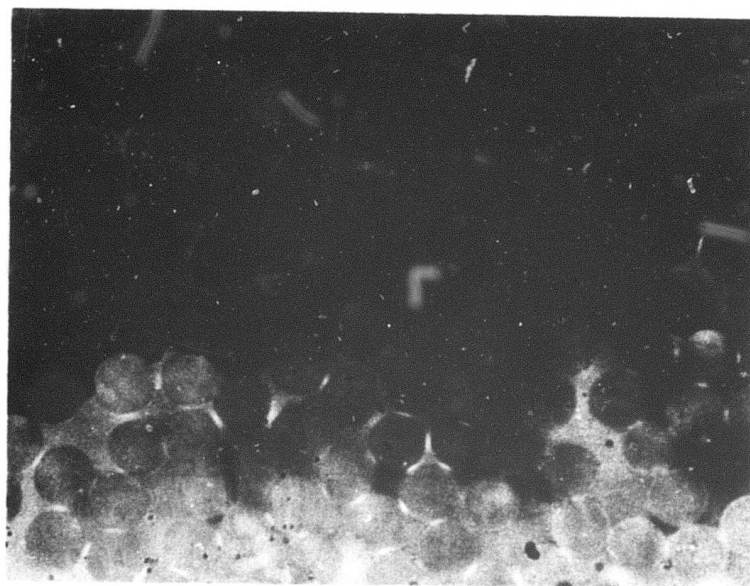


Figure 7. Polished cross-section of failed torsional fatigue specimen showing cracks for propagating around and between fibers

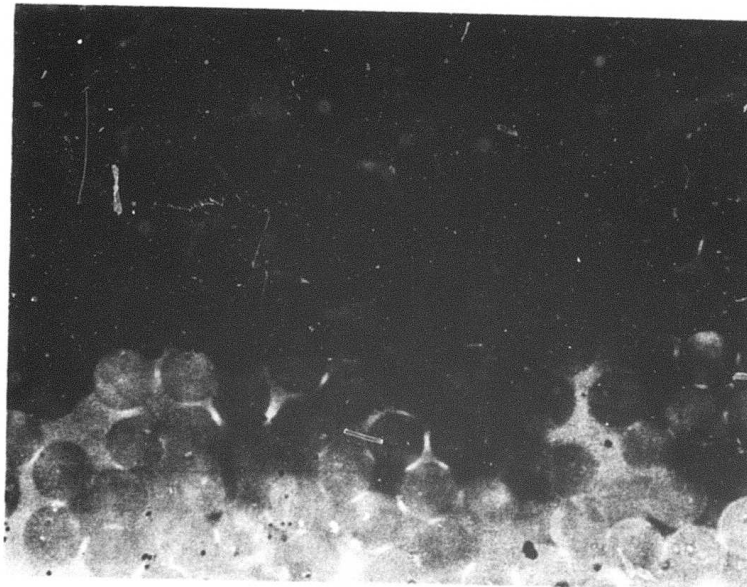


Figure 7. Polished cross-section of failed torsional fatigue specimen showing cracks for propagating around and between fibers



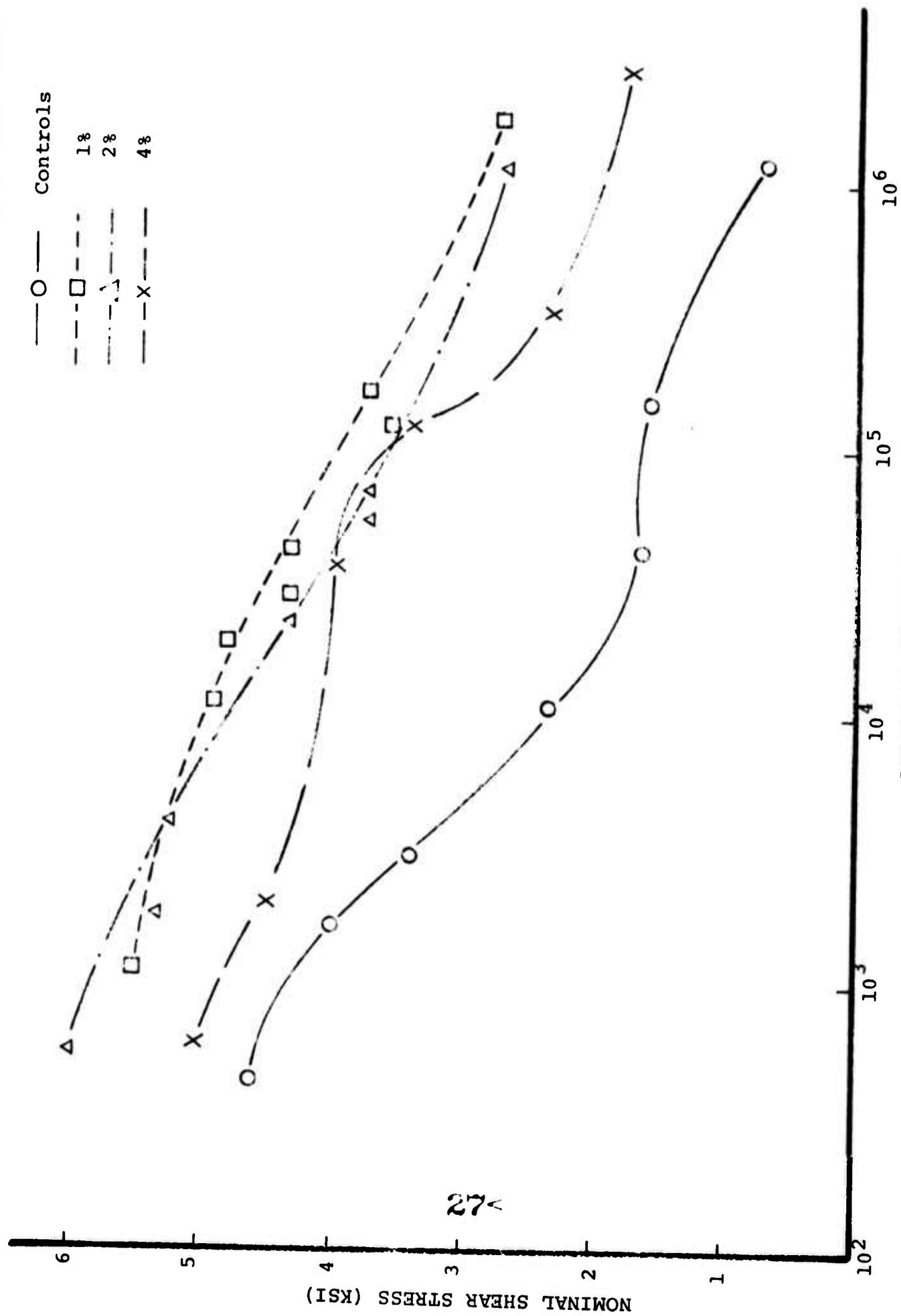


Figure 8. Torsional fatigue life vs. applied stress for glass fiber reinforced samples



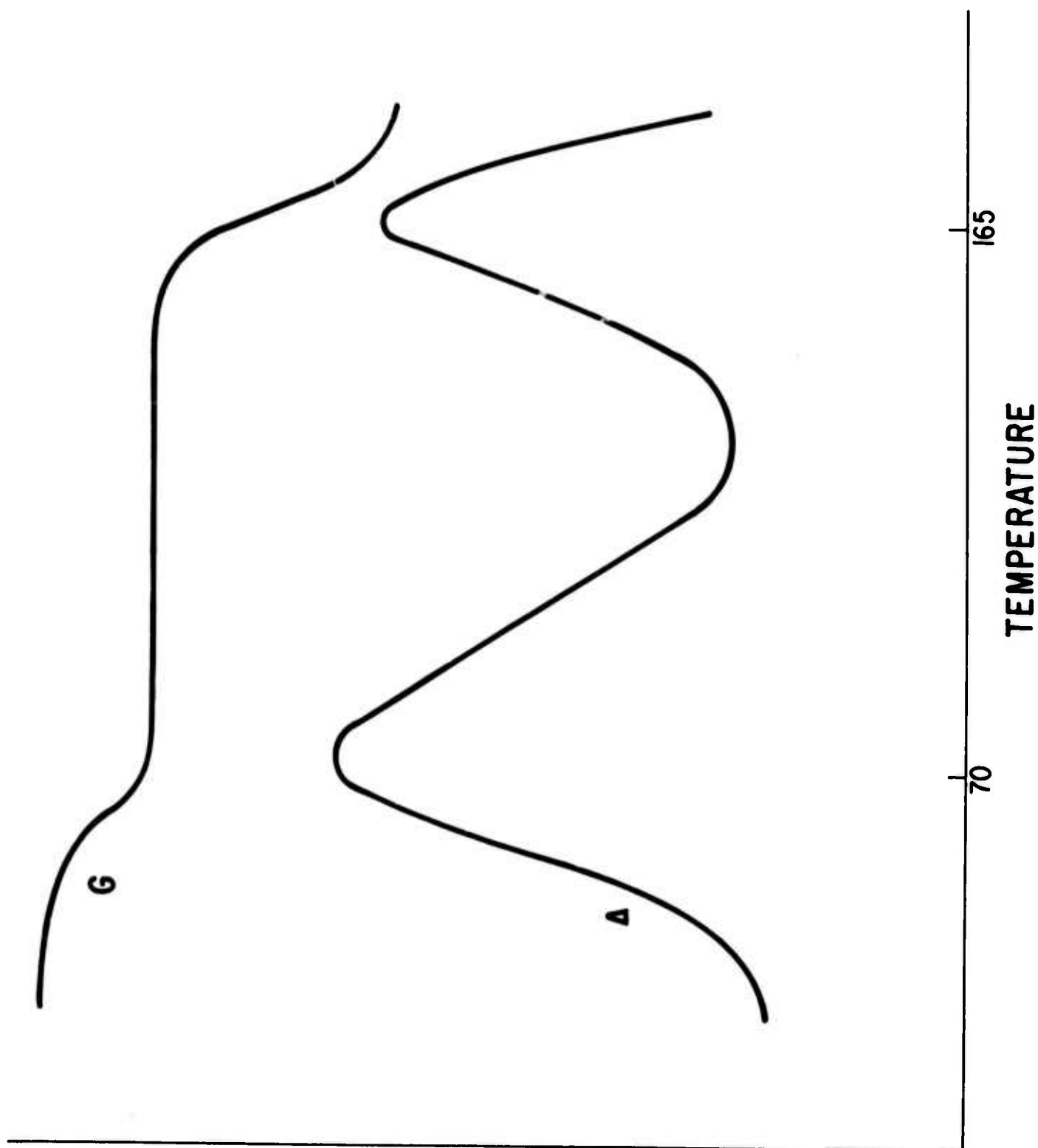


Figure 9. Dynamic modulus and damping as a function of temperature. Data were taken with a torsion pendulum at about 1 Hz.

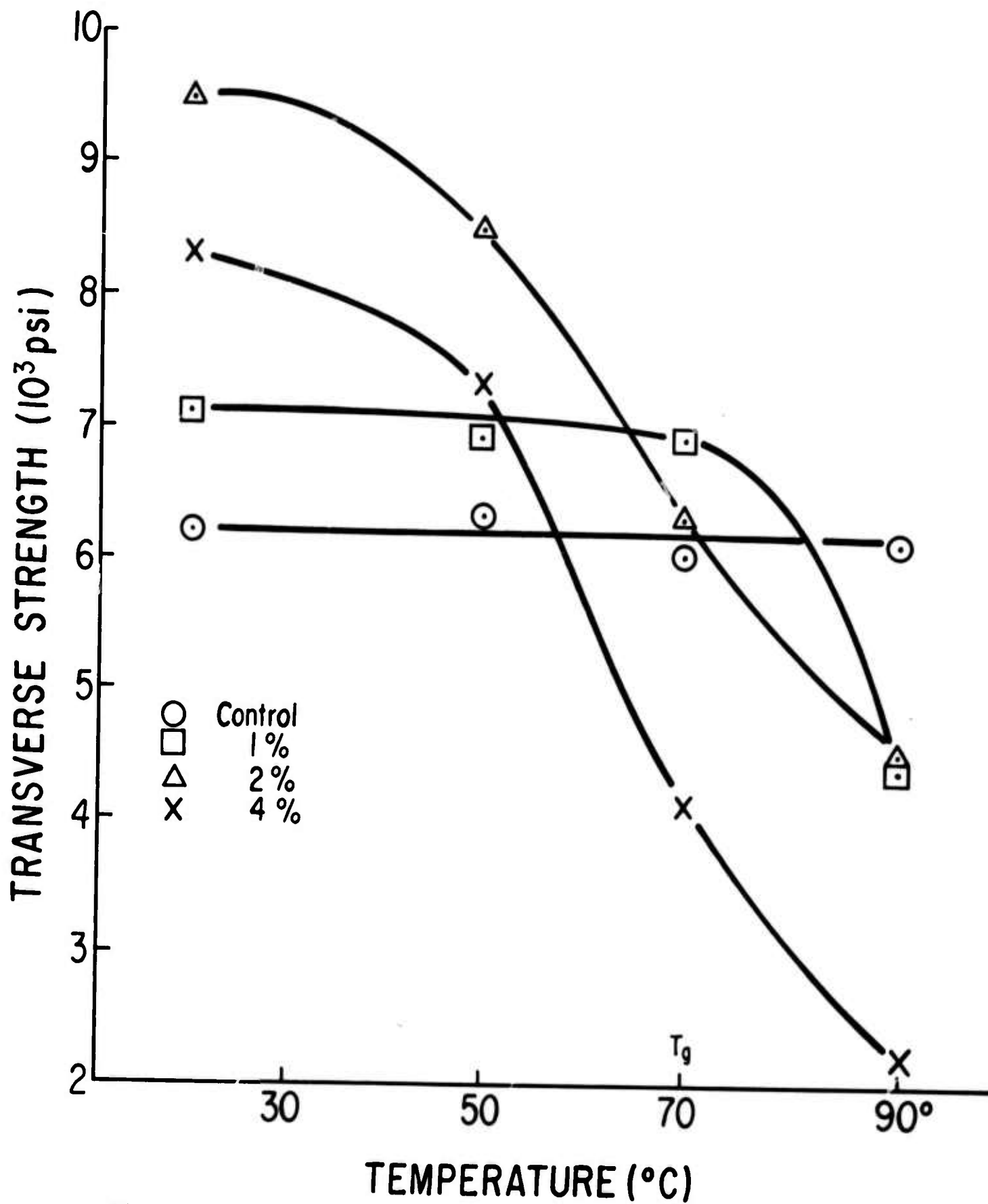


Figure 10. Transverse strength of composites at temperatures above and below the glass temperature of the innerlayer

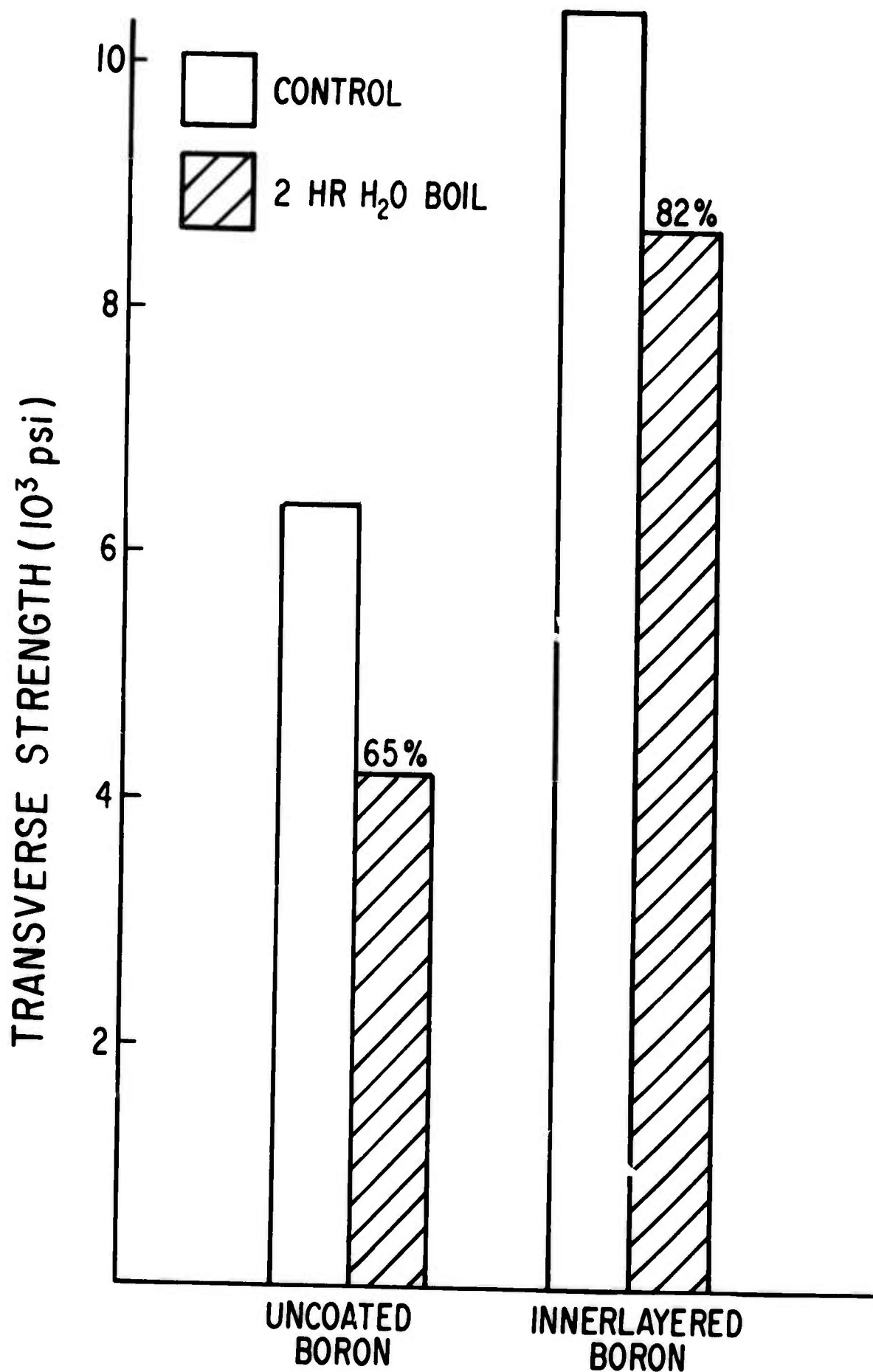


Figure 11. Transverse strength of boron fiber reinforced composites before and after 2 hours in boiling water

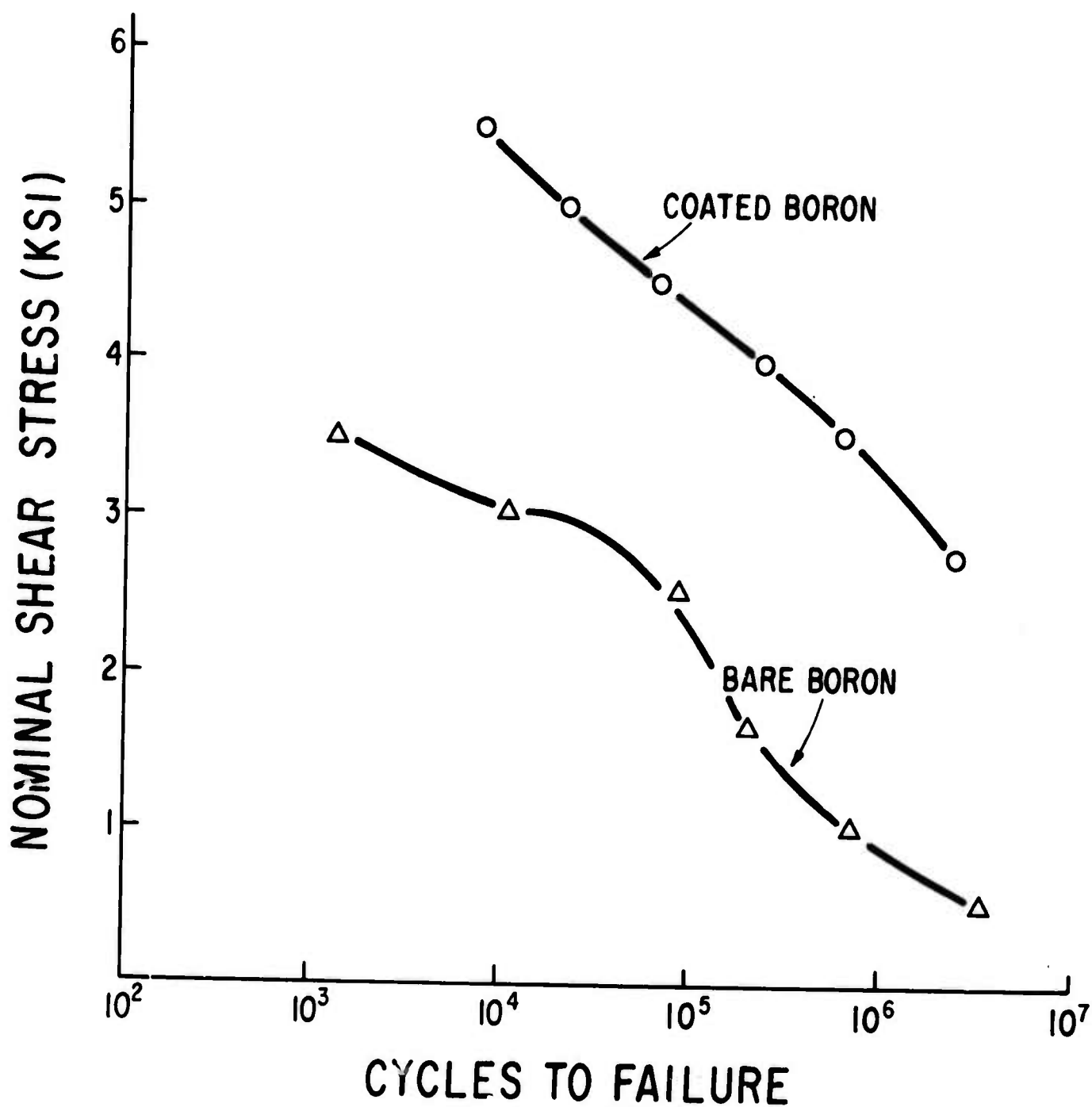
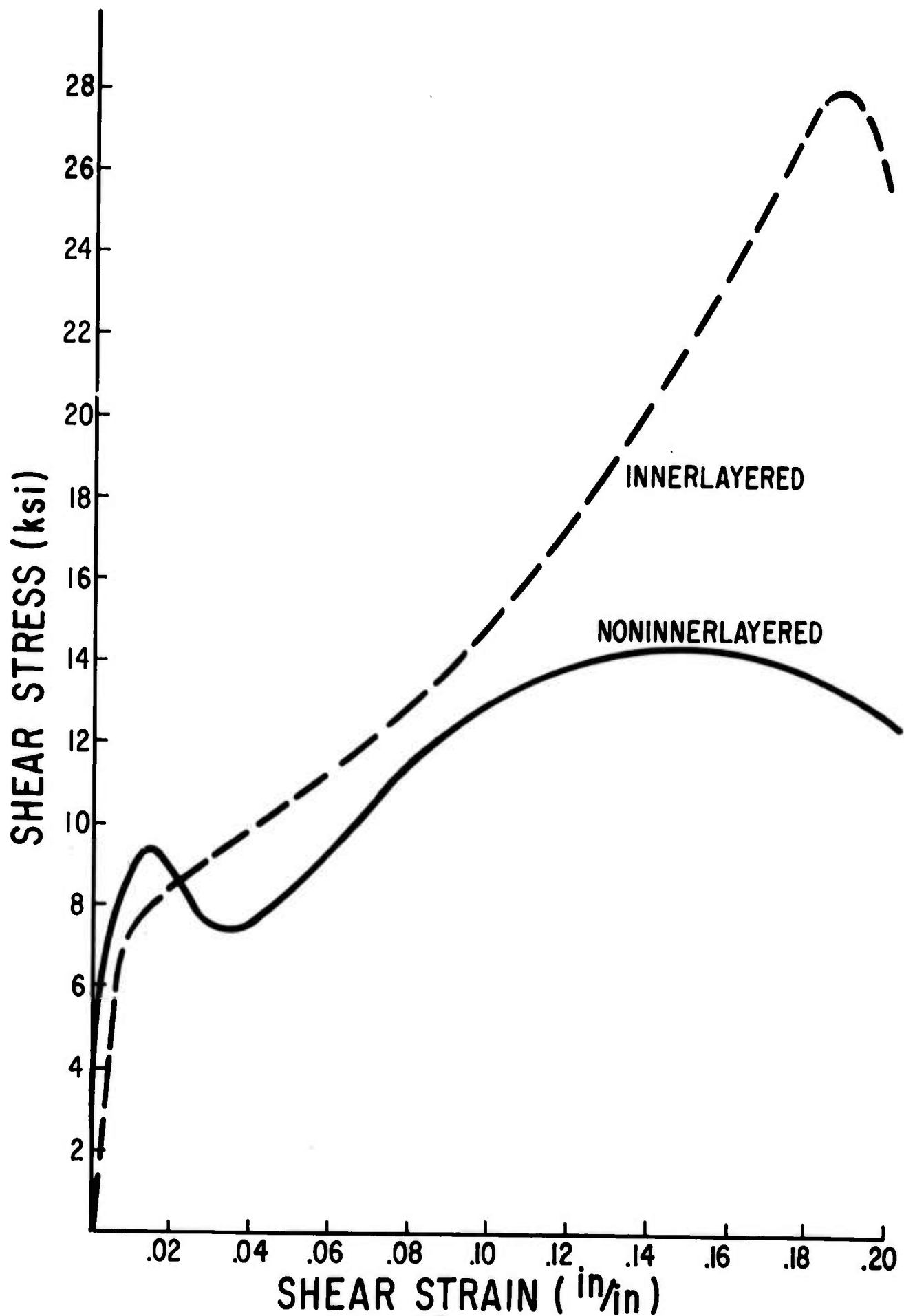


Figure 12. Torsional fatigue life vs. applied stress for boron fiber reinforced samples



32<  
Figure 13. Typical shear stress-strain curves for boron/epoxy composites.

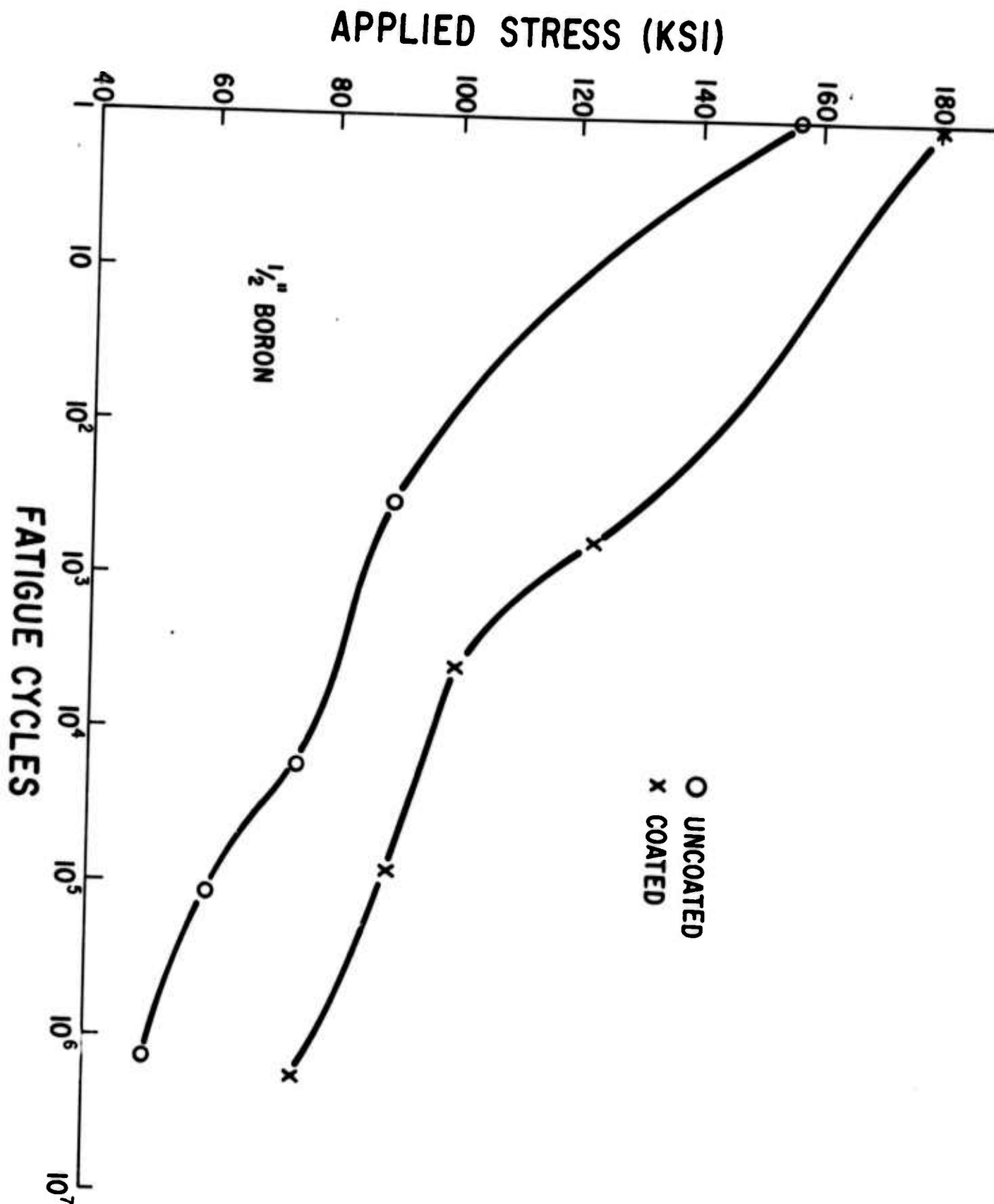


Figure 14. Flexural fatigue life vs. applied load for short boron fiber reinforced epoxy.

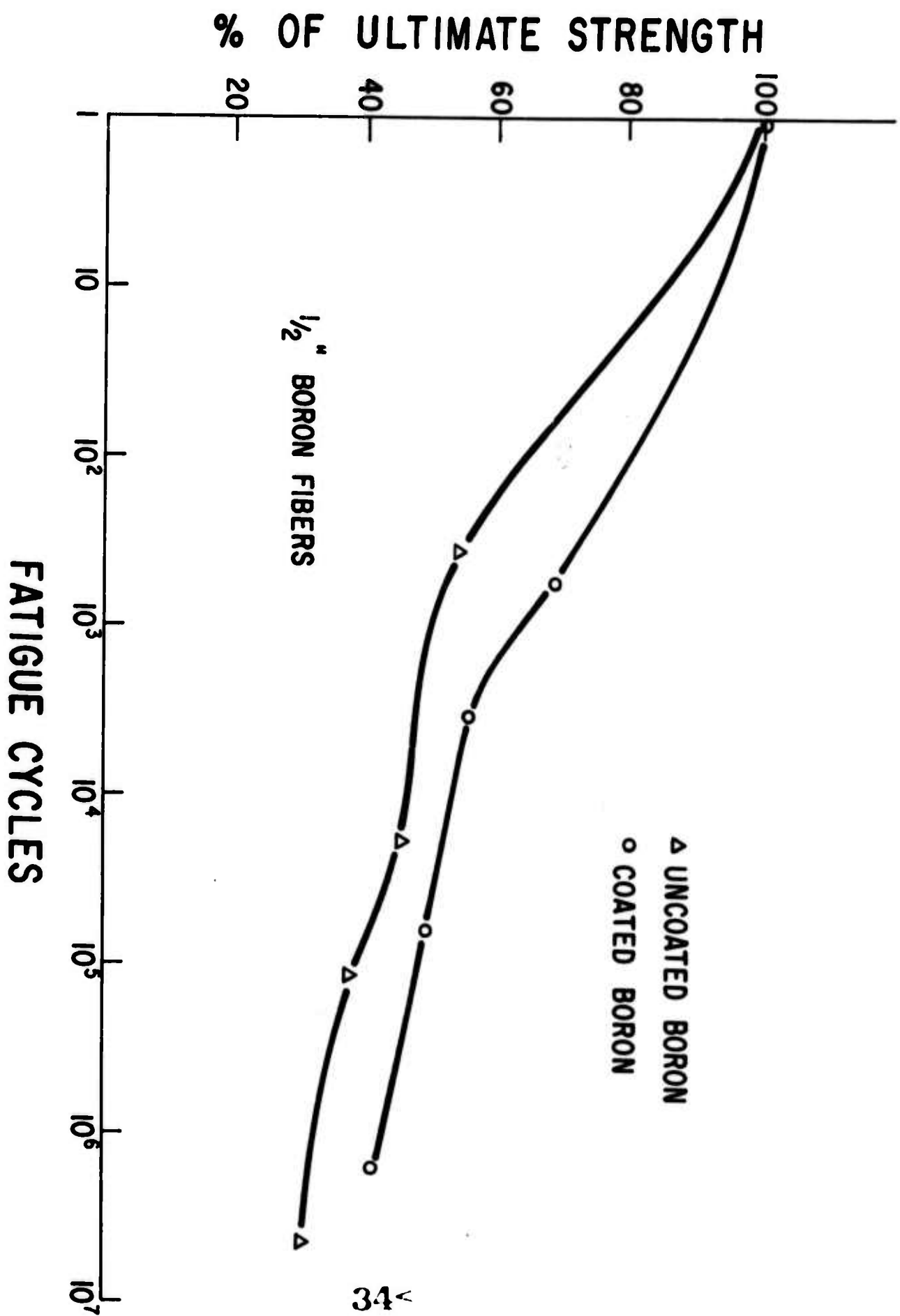


Figure 15. Flexural fatigue life vs. normalized applied load for short boron fiber reinforced epoxy.

## Appendix 1

It was initially assumed that short term, static properties in the longitudinal direction would be relatively unaffected by the presence of the flexible innerlayer. The decreased coupling between the fibers and the matrix would make the shear transfer of stresses slightly more difficult which would cause a reduction in stiffness, but strength was not expected to change significantly. Experiments designed to evaluate this loss in properties produced quite surprising results. Table 1A shows that the composites containing innerlayered fibers are all much stronger than the control specimens. This apparent anomaly was explained by subsequent measurements of fiber strength. Table 2A shows that all of the coated fibers are stronger than the uncoated ones. In the extreme cases there is more than a factor of two difference.

It is known that the strength of glass fibers is controlled by surface flaws. The above result therefore suggests that the presence of the epoxy coating may be reducing the stress concentrations around these flaws. No support for such a hypothesis could be found in the literature so the following, admittedly crude, experiments were run to evaluate the concept. A group of microscope slides were carefully removed from the package and tested in three point flexure. Another batch of slides were scratched, perpendicular to their length, with a diamond scribe under fixed weight loading. Half the slides,



selected at random, were tested with the scratch positioned at the point of maximum tensile stress. The remainder were coated with an epoxy/solvent solution similar to that used with the V-2 innerlayer. Heat was applied to drive off the solvent and a silicone coated cover glass was clamped over the scratch. After the epoxy had been cured in a 170°C oven, the cover glasses were removed. The resulting increase in the thickness was on the order of 0.2 mils. These samples were tested like the others. The results tabulated in Table 3A1 show that scratching reduces the strength to one third of the original. Applying the coating to the scratched slides doubles their strength. Similar coatings on unscratched slides show no effect on strength. This supports the hypothesis that filling a surface flaw with a low modulus material can significantly reduce the stress concentration around the crack.

A finite element model was subsequently developed to permit more detailed study of the stress fields in an innerlayered fiber. The 75 ksi strength of the original fibers indicates that the surface flaws are in the range of 10 to 100 angstroms deep. A crack length of 50 angstroms was assumed for the model. A uniform displacement was applied far from the vicinity of the crack and the stresses were mapped. Perturbations induced by filling the crack, with low modulus materials, were studied. Figure 1A shows the relative strain energy as a function of distance from the crack tip for cracks which are unfilled, filled with 815/V-140, and filled with 828/Z. At a distance of one crack length from the crack tip, there is no influence of

the fillers. Near the tip, however, both of the filled cracks have much lower stress concentrations than the unfilled one. The 815/V-140 causes a 19% decrease while the 828/Z results in a 34% decrease. The two most significant parameters in this model were the width of the crack and the modulus of the filler. Reducing the crack width or increasing the modulus causes a reduction in the stress concentration about the crack. When a fiber containing a surface flaw is loaded in tension, there is a tendency for the crack to open. Placing any sort of adhesive material in the crack provides a resistance to this opening, thereby lowering the stress concentration. The amount of reduction depends on the modulus of the filler and the width of the crack.

A series of high-strength boron fibers were also tested with and without epoxy innerlayer. In this case the innerlayer had no effect on fiber strength. The strength without a coating was 458 ksi compared to 468 ksi with the coating. This difference is not significant at the 90% level. From previous experience we know the morphology of the boron fiber is such that it has internal planes of weakness oriented perpendicular to the fiber axis. It is therefore reasonable that the fracture taking place on these planes of weakness would not be affected by a low modulus coating over the outside of the fiber. The main import of this observation is that weak fibers, or weak brittle materials, can be improved by a low modulus coating,

whereas stronger materials whose strength is not limited by surface flaws will not be improved.

An additional attribute of innerlayered fibers is that self-abrasion is greatly reduced. This was demonstrated with a series of tests on deliberately abused fibers. These were placed in a pan as if to make a continuous fiber sample. They were then worked vigorously with a spatula to cause them to rub each other. The deleterious effects of such handling are shown in Table 4A1. The control samples lost nearly one fourth of their strength, while the coated fibers were relatively unaffected.

The combined effects of reducing auto-abrasion and reducing the stress intensity around surface flaws make the composites with coated fibers much stronger than the control specimens. It should be emphasized, however, that merely coating the fibers does assure impregnation of the critical flaws. The fibers in the control specimens were obviously coated with the matrix resin (i.e., 828/Z). The rigid innerlayered fibers are also coated with the same resin, however, in this case the resin was applied in a very dilute solvent solution and cured at an unusually high temperature. The fifty percent increase in composite strength with coated fibers emphasizes the importance of wetting and impregnation.

It is difficult to assess the importance of this strengthening mechanism. For years there have been efforts to use large diameter glass fibers to produce composites with higher compressive strengths. These special materials are not generally useful because of the correspondingly low tensile strength. Perhaps with an optimized coating, the tensile strength of such composites could be improved enough to extend the usefulness of these potentially cheaper materials. Another aspect which should be investigated is the possibility of impregnating the surface flaws of weak brittle materials with a monomer and then polymerizing in situ. This would enhance the impregnation and could lead to very significant strength improvements.

### List of Tables

- Table 1A1     Average flexural strength of continuous fiber composites. The indicated range is the 90% confidence band on the average strength.
- Table 2A1     Tensile strength of glass fibers with various coatings. The range indicates the 90% confidence interval on the average.
- Table 3A1     Flexural strength of microscope slides.
- Table 4A1     Tensile strength of glass fibers before and after auto-abrasion. Only the losses of the control samples and those with Z-2 fibers are significant at the 90% level.

Table 1A1

Fiber Type	Flexural Strength of Composites (KSI)
Control	107 $\pm$ 3.0
V-1	157 $\pm$ 8.4
V-2	163 $\pm$ 2.9
V-4	137 $\pm$ 9.1
Z-2	162 $\pm$ 2.3

Table 2A1

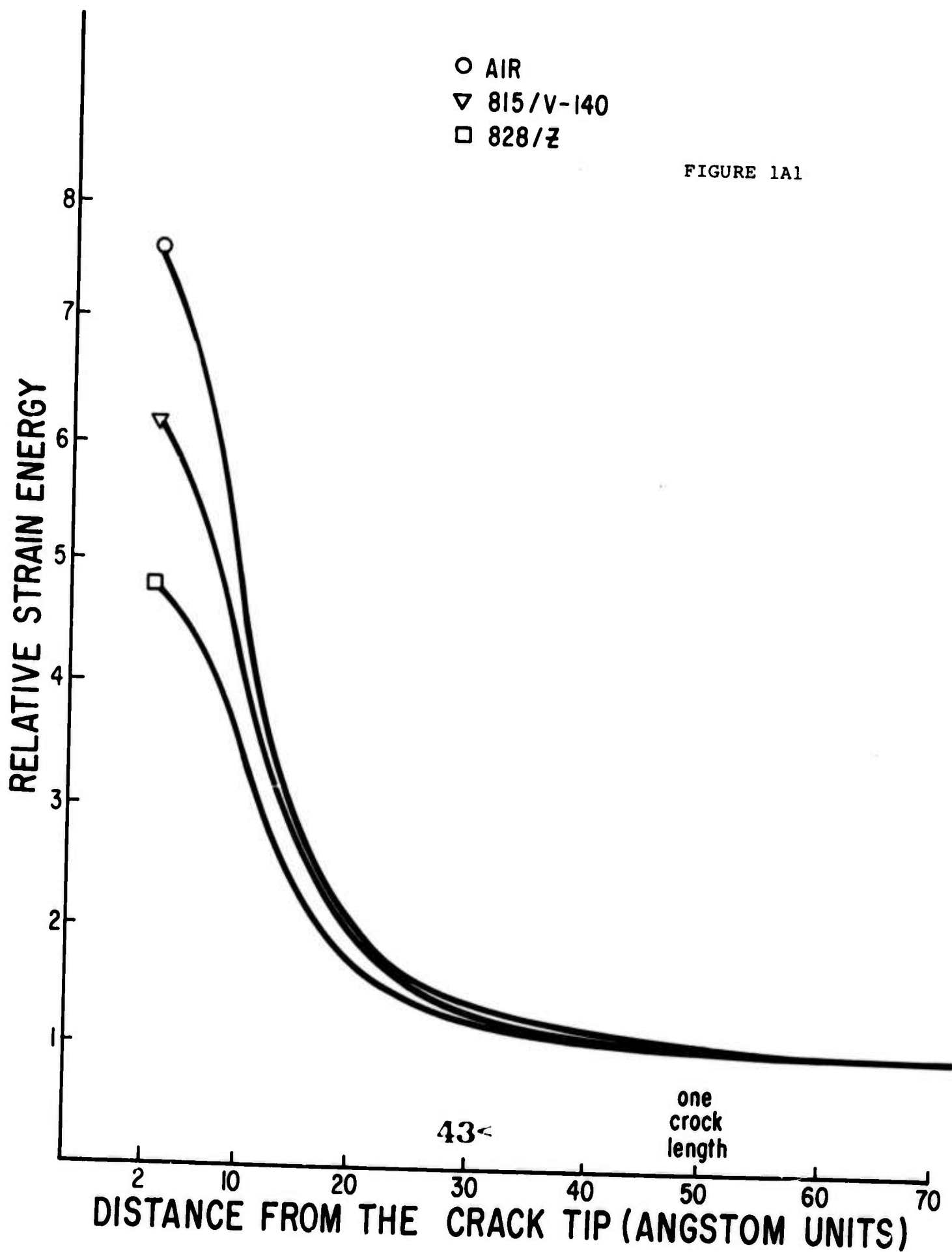
Fiber Type	Fiber Tensile Strength (KSI)
Control	72.0 $\pm$ 8.3
V-1	77.0 $\pm$ 8.9
V-2	87.6 $\pm$ 9.5
V-4	119.0 $\pm$ 12.3
Z-2	151.0 $\pm$ 16.2

Table 3A1

Flexural Strength (PSI)	
Not scratched	16,260
Scratched	4,975
Scratched and coated with 815/V-140	10,720

Table 4A1

Fiber	Tensile Strength (KSI)		Loss in Strength
	Original	Abraded	
Control	72.0 $\pm$ 8.3	54.5 $\pm$ 3.1	24.3%
V-1	77.0 $\pm$ 8.9	75.0 $\pm$ 6.7	2.6%
V-2	87.6 $\pm$ 9.5	85.5 $\pm$ 8.5	2.4%
V-4	119.0 $\pm$ 12.3	113.0 $\pm$ 13.3	5.0%
Z-2	151.0 $\pm$ 16.2	134.0 $\pm$ 15.8	11.3%





## Appendix 2

### MICROSCOPICAL TECHNIQUES FOR CHARACTERIZING INTERLAYERS IN COMPOSITE MATERIALS

John D. Fairing

In order to successfully fabricate composite materials having an interlayer between the reinforcing fibers and matrix, information on the nature of the interlayer was needed.

Described below are methods used to assess the following:

- (1) the uniformity of the interlayer applied to continuous fiber prior to fabrication of the composite;
- (2) characterization of the interlayer after the fibers are embedded in a matrix;
- (3) qualitative determination of the adhesion between the interlayer and fiber, and between the interlayer and matrix.

The two techniques employed to the largest extent were optical and scanning electron microscopy. Optical microscopic observation of stained interlayer on glass fibers provided information on the continuity and uniformity of the coating. After the fibers were combined with the polymer matrix, the scanning electron microscope was used to investigate the coating with polished cross sections which had been etched with an oxygen plasma. Fracture surfaces of static strength and fatigue test specimens were also observed with the scanning electron microscope.

A staining technique is required to make the coating visible on the glass fiber surface.

The requirements for the staining technique were:

- (1) Dye should be specific for the particular interlayer and not stain bare or sized glass;
- (2) Staining process should cause no damage or distortion of the interlayer;
- (3) The optical extinction coefficient should permit observation of less than  $0.25\mu$  in thickness.
- (4) A short period for staining.

The flexible interlayer contained more than the stoichiometric amount of curing agent, so there was an excess of free amino groups. Thus, the amino functionality was the primary candidate for dye attachment, and acid fuchsin met all of the requirements for the dye. To achieve active staining an acid dye bath of sodium bisulfate was used.

The following 4-step staining procedure was developed for the flexible interlayer:

1. The fibers were stained for 10-15 minutes at  $80-90^{\circ}\text{C}$  in a 2% aqueous solution of acid fuchsin containing 1% sodium bisulfate.
2. The fibers were washed in several changes of distilled water until all excess dye was removed (~ 30 seconds).
3. The fibers were blotted dry on bibulous paper.
4. The fibers were then mounted on a microscope slide using a mounting medium of the same refractive index as glass (e.g., "preservaslide" or Canada Balsam).

This technique stains the flexible interlayer a brilliant scarlet while imparting no color to bare or silane treated glass. Stain penetration is good, thus color intensity is a function to film thickness. Model experiments with interlayer coated glass microscope slides showed a linear dependence of color intensity on thickness to ten microns. A stained specimen of glass fiber is shown in Figure 1 with a nonuniform coating along the fiber length.

During the period when methods for applying the interlayer were being developed, many of the coatings were only partially cured. Such a coating is easily distorted and damaged during staining, and thus it was difficult to distinguish between the uniform partially cured coating, and a fully cured non-uniform coating.

The rigid interlayer was more difficult to stain than the flexible epoxy coating. The surface of the rigid interlayer may be stained to a moderate degree with Bordeaux Red substituted for acid fuchsin when the sodium bisulfate concentration is increased to 10% and the time is extended to 30 minutes. This stain shows the distribution and continuity of the resin, but because of poor penetration, does not accurately represent the thickness.

Since the innerlayer is intended to improve the mechanical properties of fiber reinforced composites, it is also important to characterize the innerlayer in fabricated samples. The use of the staining technique described above for the coated fiber

evaluation was attempted, but produced unsatisfactory results. The attempts to selectively stain the innerlayer were made on sectioned samples of glass fiber - innerlayer - epoxy matrix (Shell's Epon 828, "Z" curing agent) composites.

The innerlayer was clearly identified with an oxygen plasma applied to cross sections of the composite. The plasma attacked the innerlayer more rapidly than the matrix. The relief image produced was easily observed with the scanning electron microscope. A six step procedure was used to selectively etch the innerlayer:

1. Embed an oriented portion of the sample in a suitable media (e.g., polymethylmethacrylate).
2. Grind and polish a section using standard metallographic procedures. Avoid the use of grinding compounds coarser than 600 grit which can shatter glass fibers far under the surface, thereby causing artifacts.
3. With an optical metallograph, verify that a satisfactory polish has been obtained.
4. Etch the sample in an oxygen plasma. Etching conditions may vary with specimens; typical figures are: pressure - 0.2 torr; power - 200 watts, time - 15 minutes.
5. Prepare for scanning microscopy. Gold is preferred for plating the surface.
6. Examine with the scanning electron microscope.

A micrograph of an etched composite containing a flexible interlayer is shown in Fig. 2. For the particular composite shown in this figure, two important characteristics are observed: the innerlayer has swelled substantially and there is no discontinuity at the interlayer-matrix boundary. In Fig. 3 a surface of a composite fabricated with the rigid-innerlayer coated fibers is shown. For this sample there has been no swelling of the coating, and there is a discontinuity at the matrix-innerlayer boundary.

Previously it has been shown (3,4,5) that an examination of a composite fracture surface with a scanning electron microscope can provide important information about the composite and the failure mode. The fractography indicates qualitatively that there is improved adhesion when an interlayer is incorporated on a fiber surface. However, the microscope generally does not reveal the physical existence of the layer. Figure 4 is an exception that plainly shows the boundry of the interlayer.

Fracture surfaces of composites tested in fatigue were examined extensively. These surfaces provide information on the relative adhesion between the interlayer and both the matrix and the fiber. An example of a fatigue failure is shown in Fig. 5. It can be seen that in this specimen the fracture has occurred in some places at the fiber - interlayer interface and in others at the interlayer-matrix interface.

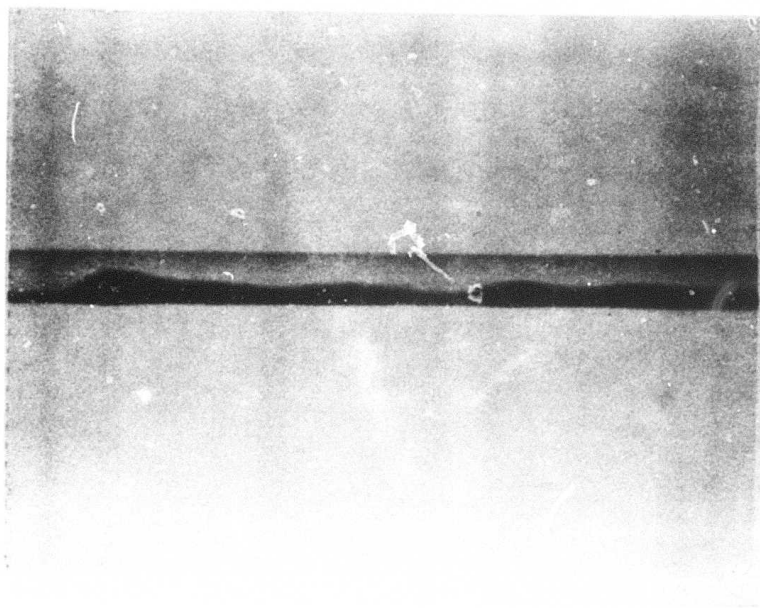
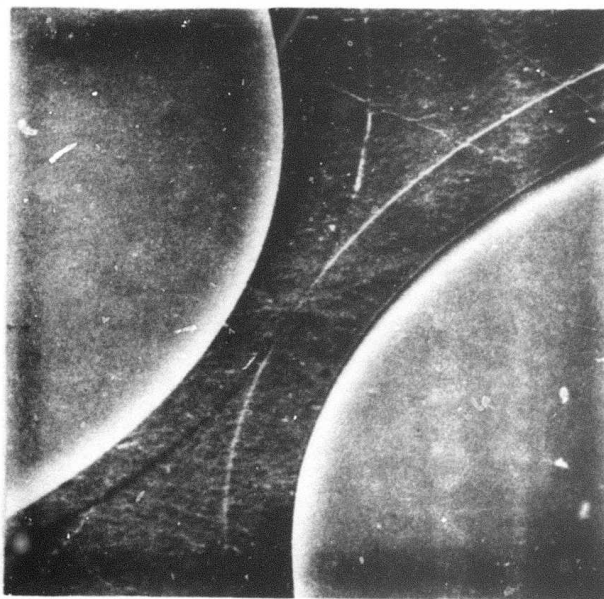


Figure 1



49<

Figure 2

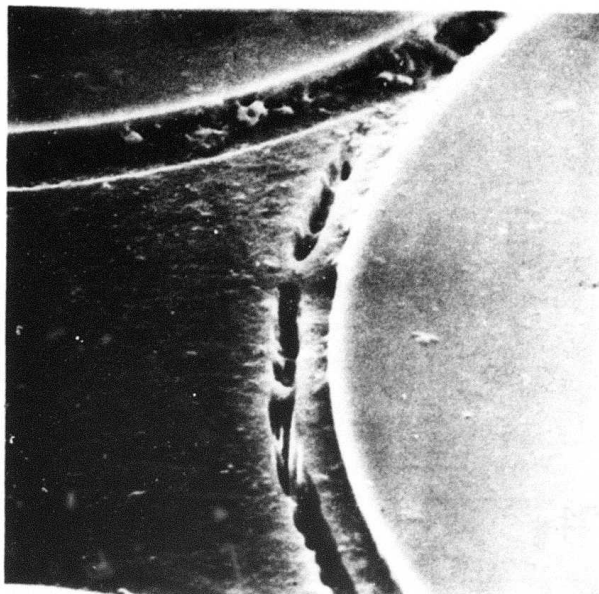
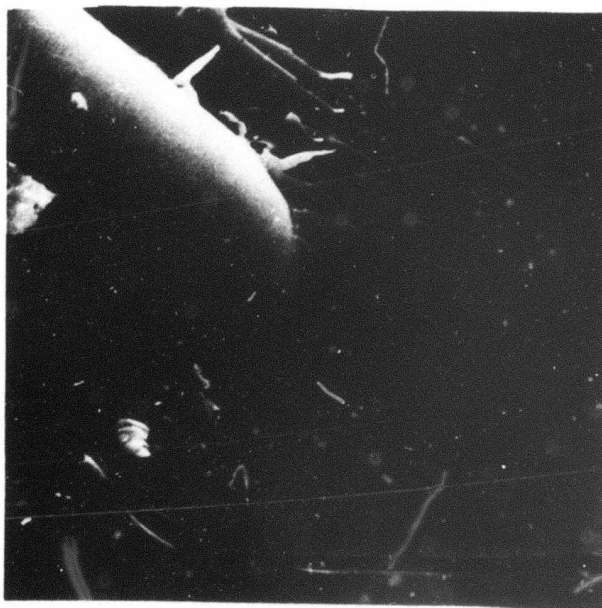


Figure 3



50<

Figure 4

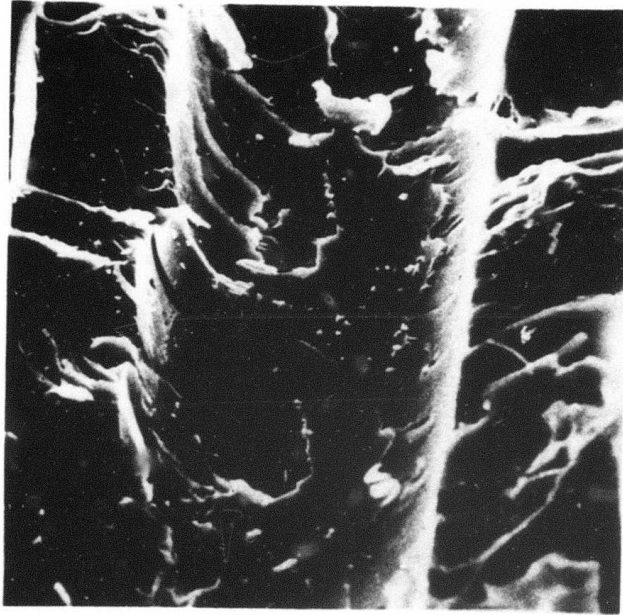


Figure 5